

CONTROL STRATEGY FOR SWITCHED RELUCTANCE MOTOR WITH ROTARY ENCODER BASED ROTOR POSITION DETECTION

Slamet RIYADI

Department of Electrical Engineering, Faculty of Engineering, Soegijapranata Catholic University, Pawiyanan Luhur IV-1, Semarang, Indonesia

sriyadi7167@gmail.com

DOI: 10.15598/aeec.v16i3.@2545

Abstract. *Development of electric drive tends to the use of Switched Reluctance Motor (SRM) for their advantages and green technology issues. The SRM takes significant place in development for its simplicity, robust construction, and low cost. Sensorless method can be applied to drive SRM, it is less expansive but has more complexity and limitation. On the other hand, although sensor-based rotor position detection needs a hardware assembled on the shaft, some advantages can be obtained. In this paper, a control strategy for SRM drive with rotary encoder based rotor position detection is proposed, core of the strategy implements digital signal controller. The problem associated with wide range speed and standstill operation can be overcome by this strategy. This is also capable to vary the time to turn the switches on and off by software. The analysis was verified by simulations and experiments.*

Keywords

Demagnetizing, freewheeling, magnetizing, rotary encoder position detection, stepping mode, switched reluctance motor.

1. Introduction

Electric drives take significant role in industry applications. They formerly use DC motors and AC induction motors. Due to the rapid progress of the power electronics and digital control developments, BLDC and SRM types of motors begin to take parts in electric drive. Green technology issues have been triggering the developments of Electric Vehicles (EV) and Hybrid Electric Vehicles (HEV) [1] and [2]. Although the torque generated by SRM is smaller than BLDC, SRM

is more interesting due to its simplicity, robustness, and low cost although it has complexities. A rotor position information is required by SRM drive to provide sequence pulses that are properly synchronized with the rotor position to achieve the required speed. In a sensor-based SRM control, rotor position detectors are commonly implemented by using Hall Effect or any other sensors. For the outputs of such sensors are time interval sectors, so it is difficult to adjust the instant time to turn on and off the switches.

In sensorless concept, no hardware is required to detect the rotor position. Some problems arise in applying this pattern so there are some limitations in such sensorless control at standstill, low and high speeds [3]. A sensorless method can use measurement of the mutually induced voltage in an inactive phase [4], derivative of the phase current [5], flux-current approach as the integration of voltage and current [6], etc.

In sensor concepts, by using Giant Magneto Resistive (GMR) sensor embedded in the air gap of the motor, the rotor position can be estimated [7]. Two SRM can be connected on the same shaft, one is operated as a motor and the other as a rotor position detector that is called Switched Reluctance Position (SRP) sensor [8]. SRM can also be operated to mimic an inductive rotor position sensor by injecting high frequency signal. This motor will act as a position sensor due to its unsaturated phase inductance [9]. A non-contact optical sensor can also be used to detect the relative position between rotor and stator at high speed [10]. Commonly, the direct rotor detections at high speed result in fluctuation in switching angles, analogue encoder can be used to synchronize the stator phase excitation and the rotor position of SRM [11].

The performance of SRM is influenced by the average torque generated, the better performance can be

obtained under larger positive torque and smaller negative torque. The instant time when the switches are turned on and off will determine the motor performance. In this paper, a control strategy for SRM using rotary encoder based rotor position detection is proposed. The proposed strategy is capable to change the points when the static switches are on and off by software. This can provide proper excitation to the stator winding so the higher average value of the torque can be generated. To verify the analysis, simulations and experiments were carried out.

2. Switched Reluctance Motor

A Switched Reluctance Motor (SRM) has very simple construction with no permanent magnet on its rotor and has simple phase winding on its stator. An equivalent circuit of SRM is shown in Fig. 1.

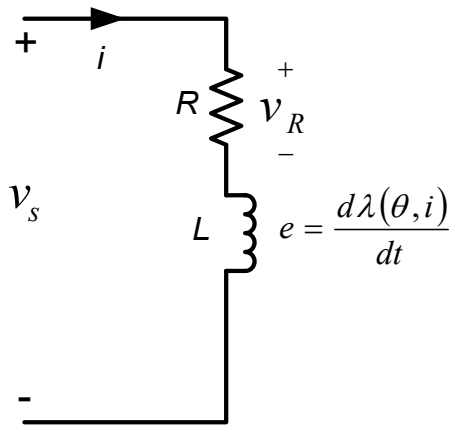


Fig. 1: Block diagram for measuring traction parameters.

To simplify the analysis, effects caused by saturation, fringing and leakage fluxes, and mutual inductance are neglected so we obtain [12]:

$$v = R \cdot i + e(\theta, i) = R \cdot i + \frac{\partial \lambda(\theta, i)}{\partial t}, \quad (1)$$

where R , i , e , θ and λ are the phase resistance, phase current, back EMF, rotor position and linkage flux. To have the power quantity, Eq. (1) must be multiplied by the current.

$$v \cdot i = R \cdot i^2 + i \cdot \frac{\partial \lambda(\theta, i)}{\partial t}. \quad (2)$$

The left-hand side term of the equation indicates the power supplied from the source while the first term of right-hand side is the ohmic dissipation and the second term of right-hand side is the sum of the mechanical power (W_m) as the output and the stored magnetic

energy (W_f). For the power is the rate of change of energy, then:

$$i \cdot \frac{\partial \lambda}{\partial t} = \frac{\partial W_m}{\partial t} + \frac{\partial W_f}{\partial t}. \quad (3)$$

If the relationship between the mechanical power (P_m) and torque (T) is defined as:

$$P_m = \frac{\partial W_m}{\partial t} = T \cdot \omega = T \cdot \frac{\partial \theta}{\partial t}, \quad (4)$$

then

$$T = i \cdot \frac{\partial \lambda}{\partial \theta} - \frac{\partial W_f}{\partial \theta}. \quad (5)$$

By using energy-coenergy concept as depicted in Fig. 2, the stored field energy (W_f) and coenergy (W_c) can be written as the following:

$$W_f = \int_0^\lambda i(\theta, \lambda) \partial \lambda, \quad (6)$$

$$W_c = \int_0^i \lambda(\theta, i) \partial i. \quad (7)$$

The area of the sum of the energy and coenergy can be declared by

$$W_f + W_c = \lambda \cdot i. \quad (8)$$

by differentiating Eq. (8), then

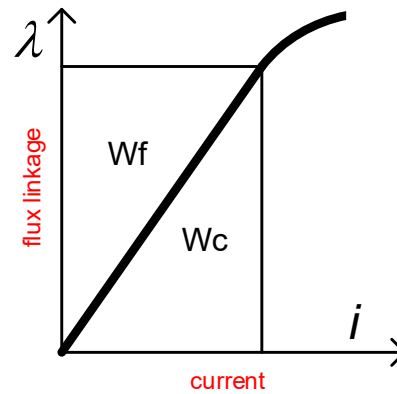


Fig. 2: The curve of energy-coenergy concept.

$$\partial W_f + \partial W_c = \lambda \partial i + i \partial \lambda, \quad (9)$$

and

$$T = \frac{\partial(-\lambda \partial i + \partial W_c)}{\partial \theta}. \quad (10)$$

Assuming the current is constant,

$$T = \frac{\partial W_c}{\partial \theta} = \frac{d \cdot \left\{ \left(\frac{1}{2} L(\theta) i \right) i \right\}}{\partial \theta}, \quad (11)$$

and finally the torque equation can be calculated as

$$T = \frac{1}{2} i^2 \frac{\partial L(\theta)}{\partial \theta}. \quad (12)$$

3. Converter Topology

A SRM with three phase stator winding and four pole rotor (6/4 SRM) requires three phase converter to generate sequential voltage waveforms to drive. Some converter topologies can be used as an electric drive. In this paper, $(n + 1)$ topology is used as a power circuit. For three phase application, this topology consists of four static switches and four diodes (Fig. 3). Three mode of operation can be implemented to operate this converter. Energizing the SRM phase stator winding can be done by switching on the upper side switch (Q_4) and one of the lower side switches (magnetizing mode). This will make the phase current increase, when the slope of the inductance profile of the appropriate phase stator is positive then the positive torque is developed (Fig. 4(a)).

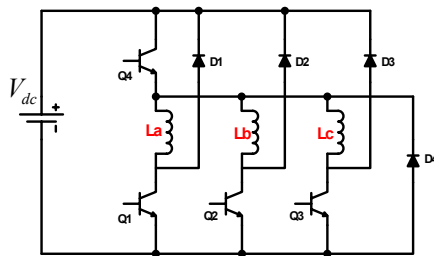
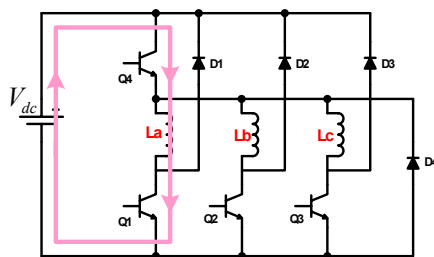
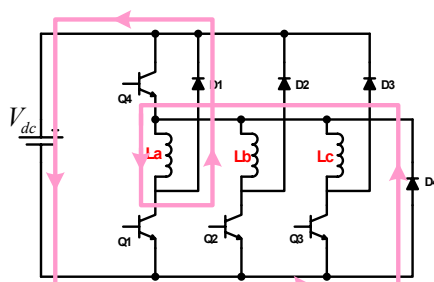


Fig. 3: Topology of $(n + 1)$ converter for 6/4 SRM.



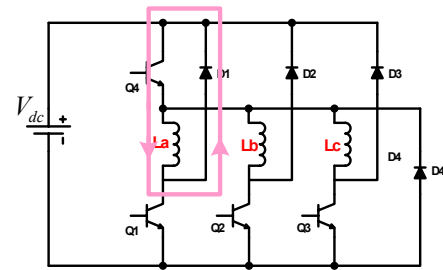
(a) The converter under magnetizing mode.



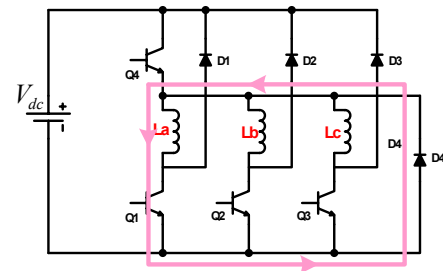
(b) The converter under demagnetizing mode.

Fig. 4: Topology of $(n + 1)$ converter for 6/4 SRM.

To turn off the current flowing in the active phase winding, two modes of operation can be used. The first mode is called demagnetizing, this make the opposite polarity of the source connected to the stator winding then the current will go down fast (Fig. 4(b)). The



(a) With upper side switch on.



(b) With lower side switch on.

Fig. 5: The $(n + 1)$ converter under freewheeling mode.

second mode is freewheeling that make the phase stator winding short circuit then the current goes down slowly (Fig. 5).

4. The Proposed Control Strategy

The proposed system consists of 6/4 SRM with rotary encoder as the detector for rotor position, a converter which is configured as the $(n + 1)$ type and a digital control as depicted in Fig. 6. By using 2000 PPR (pulse per rotation) rotary encoder and setting the unaligned position of rotor to the phase-A winding as the starting pulse, the mapping of the inductance profile due to the pulses of rotary encoder can be represented as in Fig. 7.

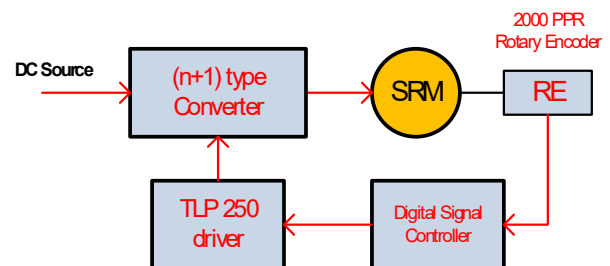


Fig. 6: The proposed drive system.

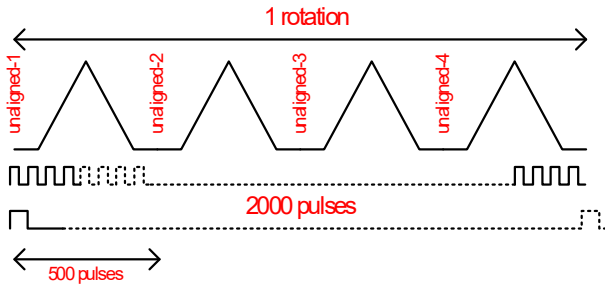


Fig. 7: Mapping of the phase-A inductance profile due to the pulses of the rotary encoder.

For the SRM has four pole rotor, it means that every unaligned position is displaced by 90 degree (mechanical degree) and represents 500 pulses of rotary encoder. If the rotor runs one rotation, there will be an inductance profile of the phase stator that repeats four times. It results in the 30 degree displacement angle between two adjacent phase winding inductance profile (Fig. 8).

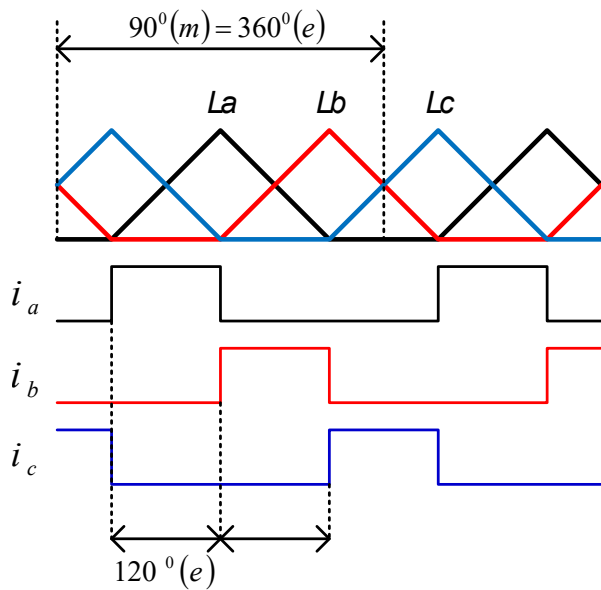


Fig. 8: Displacement angle of each phase inductance profile and ideal phase current waveforms for excitation.

If it is assumed that minimum inductance equals θ_{min} , the voltage must be applied to energize the phase-A winding at angle θ_{on} (turn on angle) and switched off at turn off angle θ_{off} where

$$0 \leq \theta_{on} \leq \frac{\theta_{min}}{2}, \tag{13}$$

$$\frac{\theta_{min}}{2} \leq \theta_{off} \leq 45^\circ \tag{14}$$

Using a rotary encoder as a rotor position detector in SRM makes the relationship between the inductance profile and the number of pulses more important. The

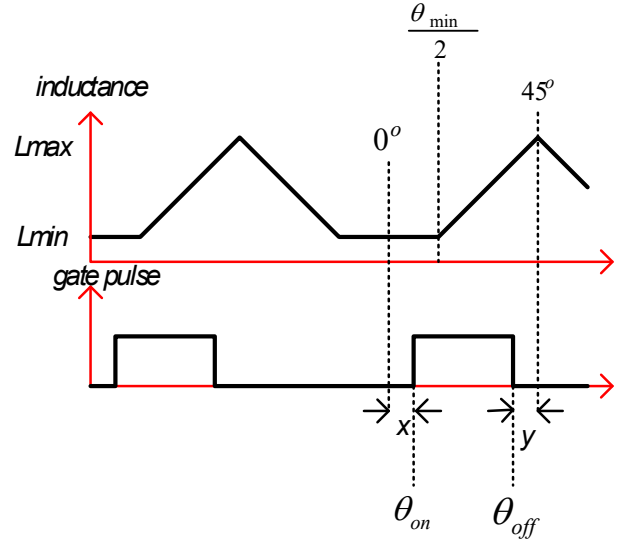


Fig. 9: Controlling the width of the pulse for the SRM drive.

number of pulses generated by the rotary encoder associated with the maximum inductance profile can be derived as:

$$A_{max}(n) = \frac{3}{6}500 + (n - 1)500, \tag{15}$$

$$B_{max}(n) = \frac{5}{6}500 + (n - 1)500, \tag{16}$$

$$C_{max}(n) = \frac{1}{6}500 + (n - 1)500, \tag{17}$$

where A_{max} , B_{max} and C_{max} are the number of the pulses generated by the rotary encoder at maximum inductance of the stator winding-A, stator winding-B and stator winding-C. In the operation of the SRM, changing θ_{on} and θ_{off} can be used to improve the performance of the motor due to Eq. (11).

Basically, to have high average value of the torque generated by the SRM, higher current should be given in the phase winding when its inductance profile slope is positive. Unfortunately due to characteristic of inductive circuit, the current is delayed to flow. Energizing the phase winding at the earlier instant time is very important to overcome the delay problem. The position of θ_{on} will determine the motor performance. When θ_{on} is too closer to 0° , there is a time interval when the current flow under zero inductance profile slope. This means the SRM absorbs the power from the source with no torque generated. But if θ_{on} is near the point $(\theta_{min}/2)$, then a the inductance profile starts to increase without adequate current value. The torque generated by the SRM under this condition may not be large enough. Different impacts arise on the placement of θ_{off} , when the switching off occurs at or greater than 45° the current remain to flow under the negative slope of the inductance profile. This results in negative

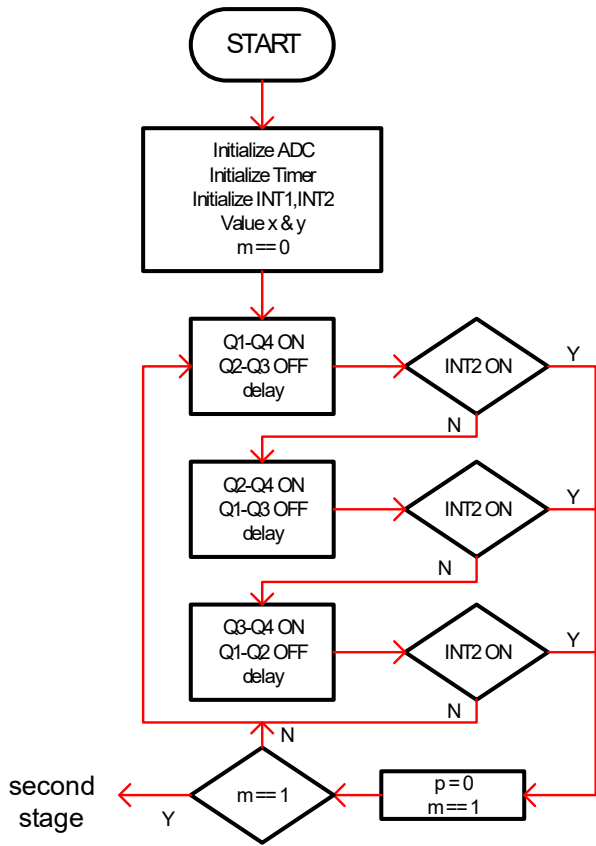


Fig. 10: Flowchart of the control strategy for the first stage.

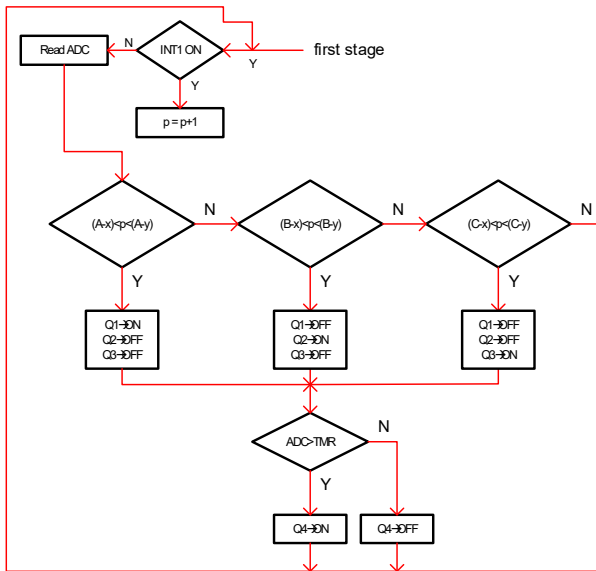


Fig. 11: Flowchart of the control strategy for the second stage with magnetizing and freewheeling operation modes.

torque produced then the average value of the torque will be low.

In designing the control strategy, the above analysis must be taken as the technical considerations. The control strategy is also capable to set the position of

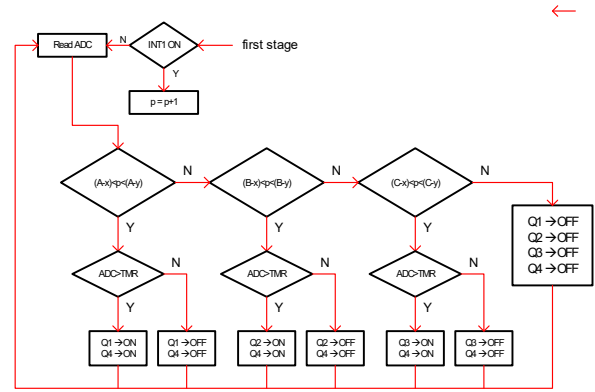


Fig. 12: Flowchart of the control strategy for the second stage with magnetizing and demagnetizing operation modes.

θ_{on} and θ_{off} to produce higher average torque. By using rotary encoder, the position of the SRM rotor can be mapped into the number of pulses generated. For rotary encoder has some outputs that represent the number pulses generated (pin A) and indicate pulses every revolution (pin Z). The Digital Signal Controller (DSC) can be implemented as the core of the control strategy. We know that the pulses generated by the rotary encoder are free running pulses so tagging the pulse as the initial position reference is required. Due to this problem, the control strategy to drive SRM is divided into two stages. The first stage is addressed to find the initial position reference by using sequence excitation given to the SRM stator windings. The rotor will start to move until the position reference obtained and then it automatically changes into the second stage that is functionalized to drive the motor.

In the first stage, the SRM is driven like a stepping motor for a moment until the pulse from pin Z of rotary encoder that connected to INT2 is generated to set the variable m that indicates that the origin pulse of pin A is started to count and is marked by the increment value of p (a variable that counts the pulses in every step in a revolution). To control the time when the switches go to on and off states by software, parameters x and y in Fig. 11 and Fig. 12 vary.

5. Results and Discussion

To validate the above analysis, computer simulations and experiments were carried out. The $(n + 1)$ converter was used in the works as the power circuit (depicted in Fig. 6). By using PSIM, simulation were performed with parameters described in Tab. 1.

The SRM speed, phase current, phase voltage and inductance profile are investigated in the simulations to prove that the control strategy is capable to change the value of the θ_{on} and θ_{off} . This can affect the SRM

Tab. 1: SRM parameters for simulation and experimental works

Resistance	0.5 Ohm
Max. Inductance	3 mH
Min. inductance	1 mH
Stator / Rotor Pole	6/4
Min. Inductance Angle	20 degree

performance especially the developed torque. Under the same load connected to the SRM, the higher torque causes higher value of the motor speed. Operating under $\theta_{on} = 0^\circ$ and $\theta_{off} = 45^\circ$ causes that the current flowing in the stator winding has high value at the time when the inductance profile begins to rise (Fig. 13). But the current is still high under negative slope of the inductance profile so the average torque is not large and finally results in low speed (Fig. 14).

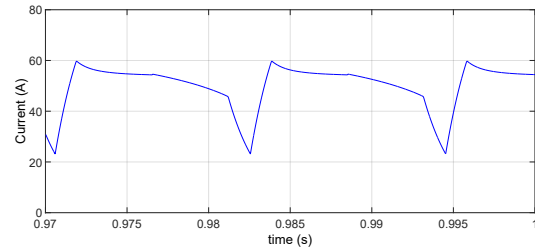
Finally, a prototype was designed to verify the proposed control strategy (Fig. 23). The 2000 PPR (pulse per revolution) rotary encoder is used to detect the rotor position. The core of the controller implements the 16 bit digital signal controller (dsPIC30F4012). The output pins A and Z of the rotary encoder are connected to INT1 and INT2 pins of the dsPIC to inform the pulses generated and the reset pulse every revolution. Parameters for this work are presented in Tab. 1. Tests of SRM with converter operated in magnetizing and freewheeling modes are depicted in Fig. 24 and Fig. 25.

Those experimental results show that the currents flowing in the stator winding tend to decrease slowly because the voltage applied on this winding is zero (freewheeling mode).

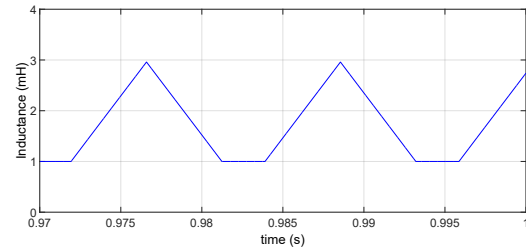
Experimental work using on equivalent to 1 pulse number ($\theta_{on} = 0^\circ$) and θ_{off} equivalent to 400 pulse number ($\theta_{off} = 360^\circ$) rotate the motor on the speed 4285 RPM as shown in Fig. 24. If the off enlarges to 500 pulse number, the lower speed is obtained (2857 RPM) as depicted in Fig. 25. Using the last parameter but the converter operated under magnetizing and demagnetizing modes results in higher speed (3864 RPM). Under this condition, the current flowing in the stator winding is drastically reduced because the voltage applied on the stator winding has negative polarity (Fig. 26).

Due to Eq. (4), under constant torque, the output power is proportional to the rotor speed. The proper θ_{on} and θ_{off} will result in higher speed and higher output power because the negative torque can be minimized, thus the efficiency is improved.

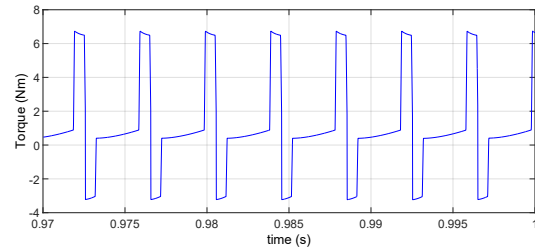
Adjusting the θ_{on} and θ_{off} by software changes the motor speed, this means that the proposed control method is effective in driving the SRM. It can be done by entering the value of x and y (Fig. 10) that represent the value of θ_{on} and θ_{off} .



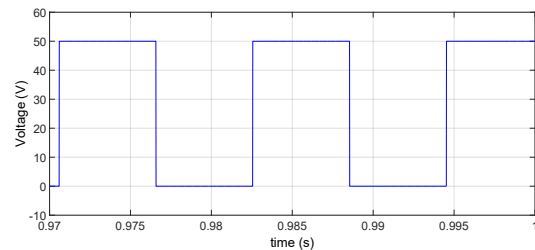
(a) Phase current.



(b) Inductance profile.



(c) Developed torque.



(d) Phase voltage.

Fig. 13: Simulation result of the SRM drive under magnetizing and freewheeling modes ($\theta_{on} = 0^\circ$ and $\theta_{off} = 45^\circ$).

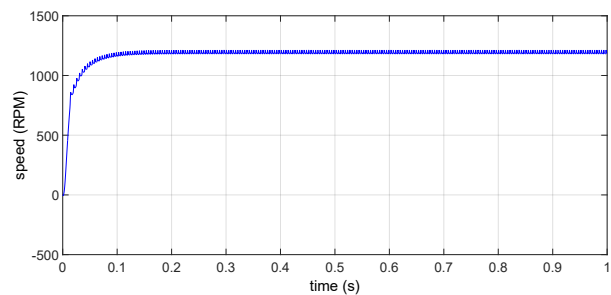
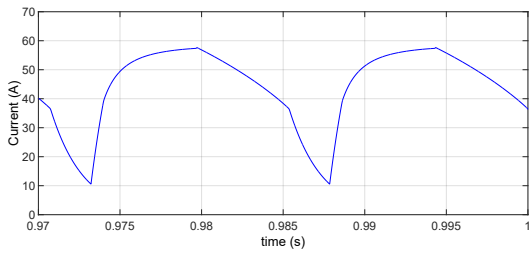
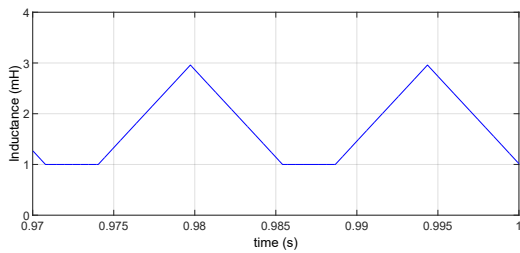


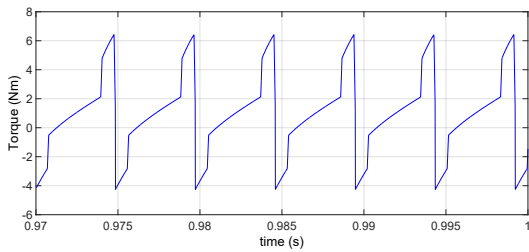
Fig. 14: Simulation result of the SRM drive speed under magnetizing and freewheeling modes ($\theta_{on} = 0^\circ$ and $\theta_{off} = 45^\circ$).



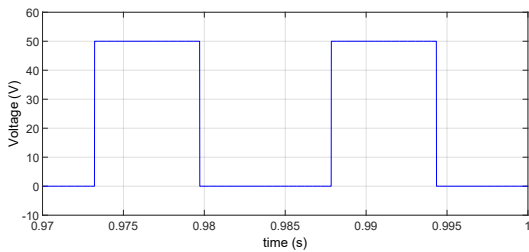
(a) Phase current.



(b) Inductance profile.

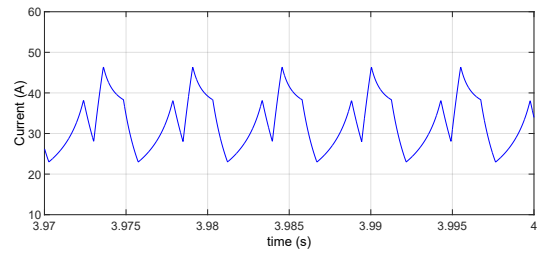


(c) Developed torque.

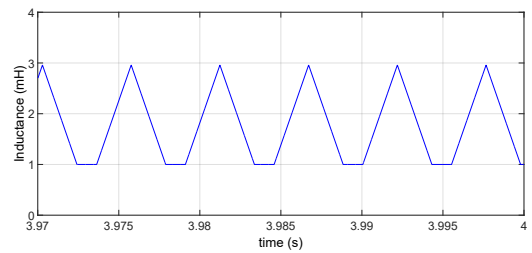


(d) Phase voltage.

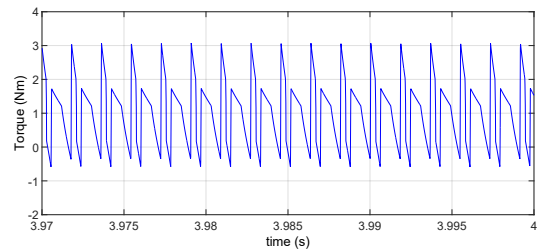
Fig. 15: Simulation result of the SRM drive under magnetizing and freewheeling modes ($\theta_{on} = 5^\circ$ and $\theta_{off} = 45^\circ$).



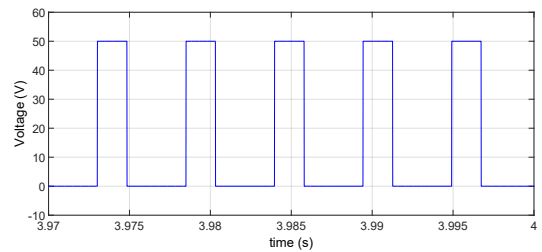
(a) Phase current.



(b) Inductance profile.



(c) Developed torque.



(d) Phase voltage.

Fig. 17: Simulation result of the SRM drive under magnetizing and freewheeling modes ($\theta_{on} = 0^\circ$ and $\theta_{off} = 30^\circ$).

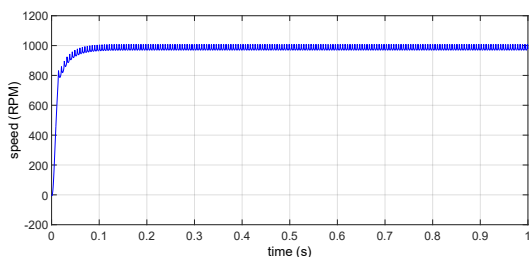


Fig. 16: Simulation result of the SRM drive speed under magnetizing and freewheeling modes ($\theta_{on} = 5^\circ$ and $\theta_{off} = 45^\circ$).

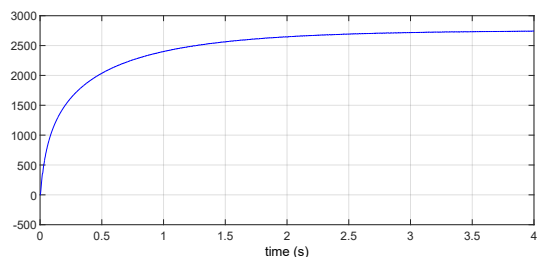
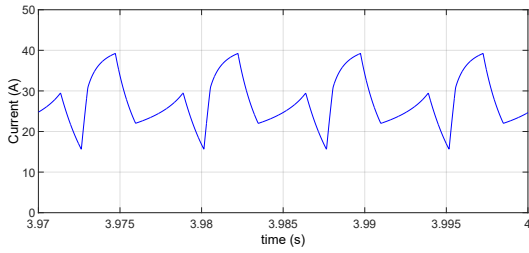
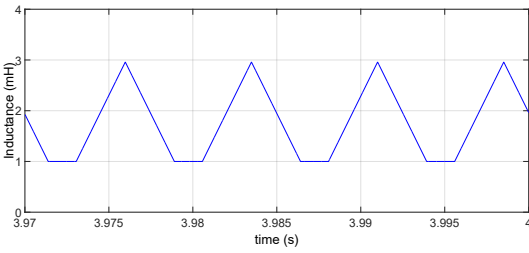


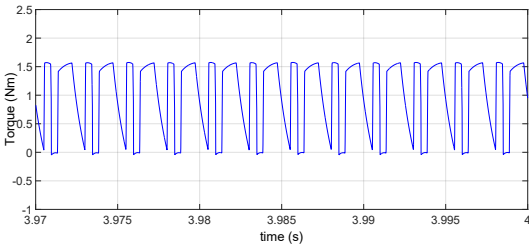
Fig. 18: Simulation result of the SRM drive speed under magnetizing and freewheeling modes ($\theta_{on} = 0^\circ$ and $\theta_{off} = 30^\circ$).



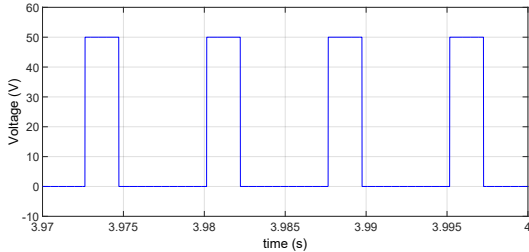
(a) Phase current.



(b) Inductance profile.

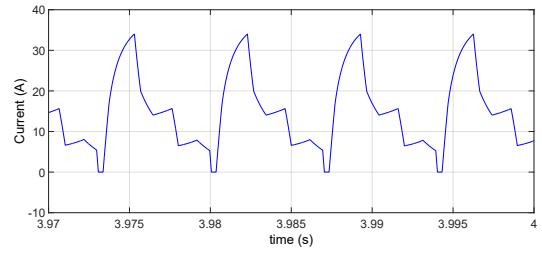


(c) Developed torque.

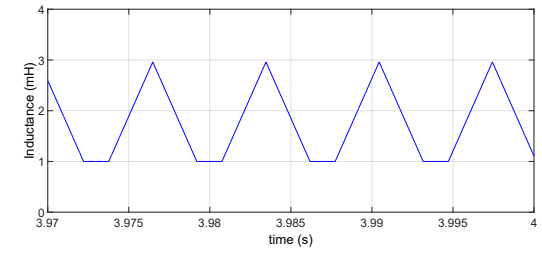


(d) Phase voltage.

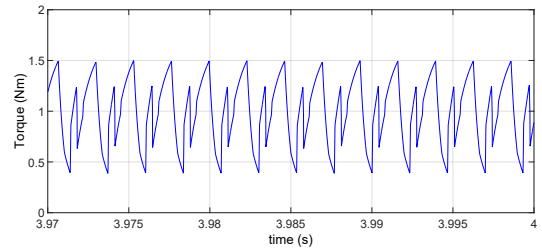
Fig. 19: Simulation result of the SRM drive under magnetizing and freewheeling modes ($\theta_{on} = 5^\circ$ and $\theta_{off} = 30^\circ$).



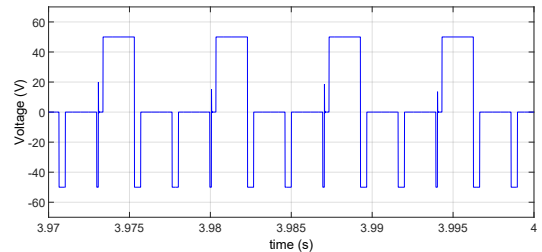
(a) Phase current.



(b) Inductance profile.



(c) Developed torque.



(d) Phase voltage.

Fig. 21: Simulation result of the SRM drive under magnetizing and freewheeling modes ($\theta_{on} = 5^\circ$ and $\theta_{off} = 30^\circ$).

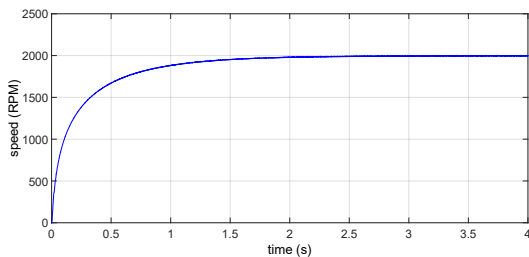


Fig. 20: Simulation result of the SRM drive speed under magnetizing and freewheeling modes ($\theta_{on} = 5^\circ$ and $\theta_{off} = 30^\circ$).

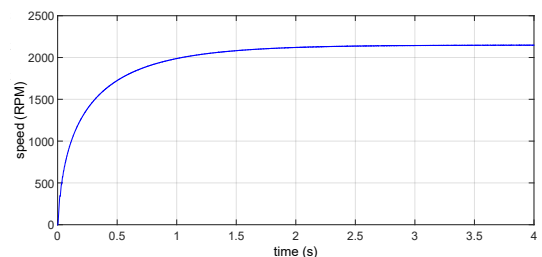


Fig. 22: Simulation result of the SRM drive speed under magnetizing and freewheeling modes ($\theta_{on} = 5^\circ$ and $\theta_{off} = 30^\circ$).

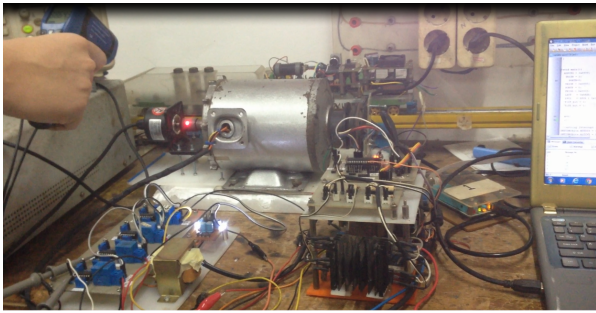


Fig. 23: The prototype for experimental works.

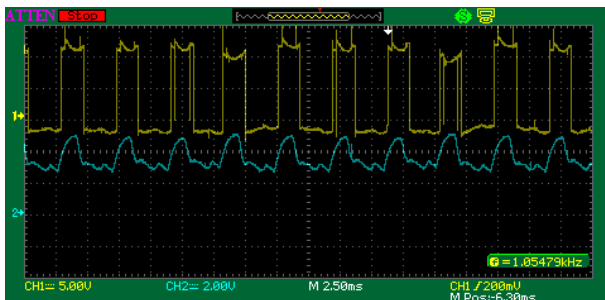


Fig. 24: Experimental result of the SRM drive under magnetizing and freewheeling modes (a) phase voltage (b) phase current (pulse number on: 0, pulse number off: 400).

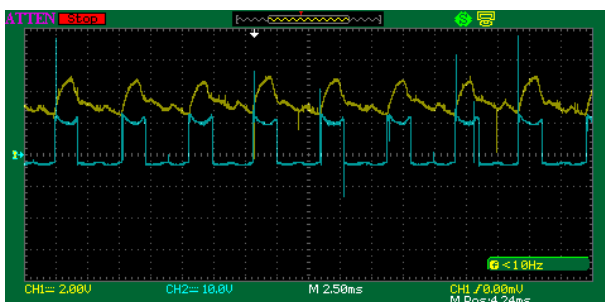


Fig. 25: Experimental result of the SRM drive under magnetizing and freewheeling modes (a) phase current (b) phase voltage (pulse number on: 0, pulse number off: 500).

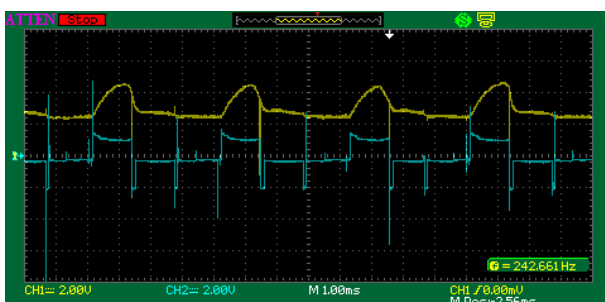


Fig. 26: Experimental result of the SRM drive under magnetizing and freewheeling modes (a) phase current (b) phase voltage 3846 RPM (pulse number θ_{on} : 0, pulse number θ_{off} : 500).

6. Conclusion

The control strategy to drive the SRM motor using rotary encoder as the rotor position detection has been presented in this paper. The strategy consists of two stages, the first stage is used to search the initial pulse number as the reference and the second stage is the main control to drive the SRM. The proposed control strategy is capable to tune the angle of turning on and turning off the switches by software so the torque produced is better. Simulations and experiments were carried out to verify the analysis and these results can prove the effectiveness of the proposed control strategy.

Acknowledgment

This work was supported by The Ministry of Research, Technology and Higher Education, Republic of Indonesia.

References

- [1] EMADI, A., Y. J. LEE and K. RAJASHEKARA. Power Electronics and Motor Drives in Electric, Hybrid Electric, and Plug-In Hybrid Electric Vehicles. *IEEE Transactions on Industrial Electronics*. 2008, vol. 55, iss. 6, pp. 2237–2245. ISSN 1000-6644. DOI: 10.1109/TIE.2008.922768.
- [2] SHAO, J. An Improved Microcontroller-Based Sensorless Brushless DC (BLDC) Motor Drive for Automotive Applications. *IEEE Transactions on Industry Applications*. 2006, vol. 42, iss. 5, pp. 1216–1221. ISSN 0093-9994. DOI: 10.1109/TIA.2006.880888.
- [3] EHSANI, M. and B. FAHIMI. Elimination of Position Sensors in Switched Reluctance Motor Drives: State of the Art and Future Trends. *Transactions on Industrial Electronics*. 2002, vol. 49, iss. 1, pp. 40–47. ISSN 0278-0046. DOI: 10.1109/41.982246.
- [4] HUSAIN, I. and M. EHSANI. Rotor Position Sensing in Switched Reluctance Motor Drives by Measuring Mutually Induced Voltages. *IEEE Transactions on Industry Applications*. 1994, vol. 30, iss. 3, pp. 665–672. ISSN 0093-9994. DOI: 10.1109/28.293715.
- [5] XU, Z. Sensorless Switched Reluctance Motor Driver System Control by Detecting the Derivative of the Phase Current. In: *The 2011 International Conference on Electric Information and Control Engineering*. Wuhan: IEEE,

- 2011, pp. 1116–1119. ISBN 978-1-4244-8036-4. DOI: 10.1109/ICEICE.2011.5777929.
- [6] PANDA, D. and V. RAMANARANAYAN. Sensorless Control of Switched Reluctance Motor Drive with Self-Measured Flux-Linked Characteristics. In: *The IEEE 31st Annual Power Electronics Specialists Conference*. Galway: IEEE, 2000, pp. 1596–1574. ISBN 0-7803-5692-6. DOI: 10.1109/PESC.2000.880539.
- [7] TRAORE, W. F. and R. A. MCCANN. Rotor Position Estimation in a Switched Reluctance Motor Using Embedded Magnetic Field Sensors. In: *The 2010 IEEE Power and Energy Society General Meeting*. Providence, RI: IEEE, 2010, pp. 1–11. ISBN 978-1-4244-6549-1. DOI: 10.1109/PES.2010.5590141.
- [8] CAI, J. and Z. DENG. Switched-Reluctance Position Sensor. *IEEE Transactions on Magnetics*. 2014, vol. 50, iss. 11, pp. 1–4. ISSN 1478-7148. DOI: 10.1109/TMAG.2014.2329957.
- [9] CAI, J., Z. LIU, H. JIA, X. ZHAO and F. XU. An Inductive Position Sensor with Switched Reluctance Motor Structure. In: *The 20th International Conference on Electrical Machines and Systems (ICEMS)*. Sydney: IEEE, 2017, pp. 1–4. DOI: 10.1109/ICEMS.2017.8056495.
- [10] GONG, C., T. HABETLER, J. RESTREPO, and B. SODERHOLM. Direct Position Control for Ultra-high Speed Switched Reluctance Machines Based on Non-contact Optical Sensors. In: *The 2017 IEEE Electric Machines and Drives Conference (IEMDC)*. Miami: IEEE, 2017, pp. 1–6. ISBN 978-1-5090-4281-4. DOI: 10.1109/IEMDC.2017.8002289.
- [11] AHN, J. W., S. J. PARK and D. H. LEE. Novel Encoder for Switching Angle Control of SRM. *IEEE Transactions on Industrial Electronics*. 2006, vol. 53, no. 3, pp. 848–854. ISSN 0278-0046. DOI: 10.1109/TIE.2006.874278.
- [12] DIRENZO, M. T. Application Report: SPRA420A. *Switched Reluctance Motor Control - Basic Operation and Example Using the TMS320F240*. Texas Instruments, 2000.

About Authors

Slamet RIYADI was born in Semarang, Indonesia. He received his B.Sc. from Diponegoro University Semarang in 1991, M.Sc. from Bandung Institute of Technology, Indonesia in 1997. In 2006, he received Ph.D. degree in Electrical Engineering from Bandung Institute of Technology with Ph.D. partial research done in ENSEEIHT-INP Toulouse France. His research interests include power converter, power quality, PV-Grid Connected System and Electric Drive. Currently he is with the Department of Electrical Engineering, Soegijapranata Catholic University Semarang Indonesia.